

Effects of Compressed Carbon Dioxide on the Phase Equilibrium and Molecular Order of a Lyotropic Polyamide Solution

Michael A. Winters,[†] Pablo G. Debenedetti,^{*,†} Peter D. Condo,[‡] Maciej Radosz,^{‡,§} and Hans-Werner Schmidt[⊥]

Department of Chemical Engineering, Princeton University, Princeton, New Jersey 08544, Corporate Research, Exxon Research and Engineering Company, Annandale, New Jersey 08801, Department of Chemical Engineering, Louisiana State University, Baton Rouge, Louisiana 70803, and Makromolekulare Chemie I, Bayreuth University, D-95440 Bayreuth, Germany

Received December 15, 1995; Revised Manuscript Received April 2, 1996[®]

ABSTRACT: The effects of compressed carbon dioxide at slightly subcritical temperatures on solutions of a chloro-substituted, para-linked aromatic polyamide (PPTA-Cl) in dimethylacetamide were investigated by depolarized light spectroscopy. Pressurization of isotropic solutions resulted in polymer precipitation at a sharply defined pressure. Pressurization of nematic solutions resulted in an increase in the intensity of scattered light with no evidence of precipitation. A plausible interpretation of this observation is the occurrence of liquid–liquid phase separation into polymer-rich (anisotropic) and polymer-lean (isotropic) phases induced by the compressed carbon dioxide. The results suggest that compressed, near-critical antisolvents can be used to control the degree of anisotropy in liquid-crystalline polymeric systems.

Introduction

An important application of liquid-crystalline polymers (LCPs)^{1,2} is in the processing of ultrahigh-strength fibers from aromatic polyamides. Kevlar, for example, is an aramid fiber produced from the wet-spinning of a nematic anisotropic solution. It is used as an antiballistic material, in automobile tires and brake pads, in mooring cables, and in fire-resistant clothing. Kevlar owes its high modulus, which ranges from 62 to 124 GPa, to competitive interactions between conjugate groups of well-ordered polyamide chains,^{3,4} and it is stronger than steel on a per mass basis. While Kevlar is only slightly denser than nylon, its tensile strength is approximately 30 times greater.⁵

In spite of the numerous applications of LCP-based systems, there is a need for improved processing routes that will enable greater control over the product's microstructure and physical properties. The avoidance of macroscopic heterogeneity (which hinders packing density and lowers the overall tensile strength of fibers) and the attainment of multiaxial order remain important goals.⁶

In this study, we investigate the effects of compressed antisolvents on the extent of orientational order in a lyotropic LCP system. Both isotropic and anisotropic phases of a chloro-substituted, para-linked aromatic polyamide (PPTA-Cl) were contacted with slightly subcritical CO₂ ($T/T_c = 0.99$) and also, for comparison, with highly supercritical argon ($T/T_c = 2.0$). The intensity of light scattered and depolarized by a thin liquid film of PPTA-Cl solution was used to monitor changes in the extent of orientational order. The results suggest that near-critical, compressed antisolvents can be used to control the physical properties of lyotropic LCP systems.

A recent study of Suresh *et al.*⁷ is of considerable relevance to the interpretation of our results. These authors investigated the phase behavior of Nylon 6 (a

nonlyotropic, flexible chain polyamide), trifluoroethanol (TFEtOH), and carbon dioxide. They found that CO₂ served as an effective diluent to lower the viscosity of the polyamide solution, while maintaining a high solubility of Nylon 6 in the resulting mixed solvent.⁷ In particular, Suresh *et al.* observed that, above 100 °C and at high CO₂ concentrations, the ternary system underwent liquid–liquid phase separation. They used the Statistical Associating Fluid Theory^{8,9} to model this phase separation. The observed and predicted phases consisted of a CO₂ phase containing some TFEtOH, a polymer-lean, CO₂-rich TFEtOH liquid phase, and a polymer-rich, CO₂-lean TFEtOH liquid phase.⁷

The use of compressed gas antisolvents is well-established for polymer separations^{10,11} and for the formation of polymer microparticles.^{12–15} Unlike liquids, near-critical fluids are highly compressible. Hence, with near-critical antisolvents, small changes in pressure can be used to cause large changes in solvent density and to induce the polymer solution to phase separate.¹¹ Furthermore, the compressed antisolvent can be removed completely by simple depressurization. Previous work^{12,13} on aromatic polyamides and compressed antisolvents was aimed primarily at studying the morphology of the precipitated polymer particles. The present study is the first one to monitor spectroscopically changes in the extent of chain orientational order in the presence of compressed antisolvents.

Traditional polyamide processing solvents are highly reactive (sulfuric acid) or possess high boiling temperatures (*m*-cresol), making solvent removal difficult.⁷ Para-linked aromatic polyamides were developed to overcome this limitation; several are, in fact, soluble in less severe solvents.^{16–18} The present results point to the practical importance of understanding the phase behavior of such lyotropic systems in the presence of compressed antisolvents such as CO₂. Relatively few studies of the phase behavior of polymer solutions and compressed CO₂ exist in the literature.^{7,19,20}

Experimental Section

Materials. PPTA-Cl, a chloro-substituted, para-linked aromatic polyamide, shown in Figure 1, was synthesized

* To whom correspondence should be addressed.

[†] Princeton University.

[‡] Exxon Research and Engineering Co.

[§] Present address: Louisiana State University.

[⊥] Bayreuth University.

[®] Abstract published in *Advance ACS Abstracts*, June 15, 1996.

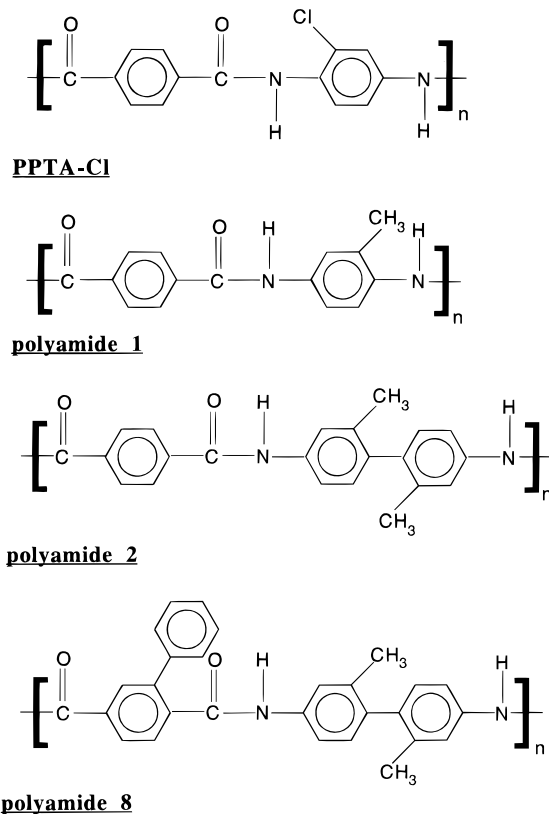


Figure 1. Chemical structures of various polyamide samples. PPTA-Cl was used in this study. The other polyamides were used in particle formation studies,^{14,15} and their precipitation thresholds are shown in Figure 5.

according to previously published procedures.²¹ Also shown in Figure 1 are other related polyamides that we have used in previous precipitation work involving compressed antisolvents.^{12,13} The polyamide had an inherent viscosity of 1.72 dL/g in 96 wt % H₂SO₄ at 35 °C.

Two solutions of PPTA-Cl in anhydrous *N,N*-dimethylacetamide (DMAc) were explored. Prior to dissolving the PPTA-Cl, lithium chloride salt (LiCl) was added to the DMAc to form a 4.0 wt % solution. LiCl increases the solubility of the PPTA-Cl in DMAc due to the association of chloride ions with amide protons in the polymer.²² The first solution, containing 3.0 wt % PPTA-Cl, was isotropic. The second solution contained 11 wt % PPTA-Cl and was biphasic; the denser phase exhibited nematic anisotropy at ambient temperature and pressure. For this polyamide in DMAc/LiCl, phase separation into polymer-rich (anisotropic) and polymer-lean (isotropic) phases occurs above 7.0 wt % PPTA-Cl at ambient *T* and *P*.²¹

Additional experiments were conducted with solutions of 20 wt % PPTA-Cl in 4.0 wt % LiCl in DMAc. The turbidity of these highly concentrated, lyotropic solutions limited the ability to measure changes in the intensity of scattered light. Furthermore, due to the high concentration of polymer, it was difficult to differentiate between liquid–liquid phase separation and polymer precipitation.²³

DMAc (99.95% purity, Lot 01219kv) was purchased from Aldrich Chemical Co. (Milwaukee, WI). LiCl (low sodium, Lot No. D29333) was purchased from J. D. Baker, Inc. (Phillipsburg, NJ). Argon (99.9% purity) and bone-dry grade CO₂ (99.8% purity) were purchased from Matheson Gas Products (East Rutherford, NJ).

Apparatus and Procedure. The experimental apparatus, shown in Figure 2, consisted of a high-pressure optical cell, a helium–neon laser, Glen-Thompson polarizers, a photodetector and photomultiplier, and a pressurization system.

The stainless steel cell (316SS) shown in Figure 3 was manufactured by General Machine Craft, Inc. It is rated to withstand pressures of up to 1700 bar and has a cylindrical-shaped internal cavity, 15.2 mm in diameter × 41.2 mm in

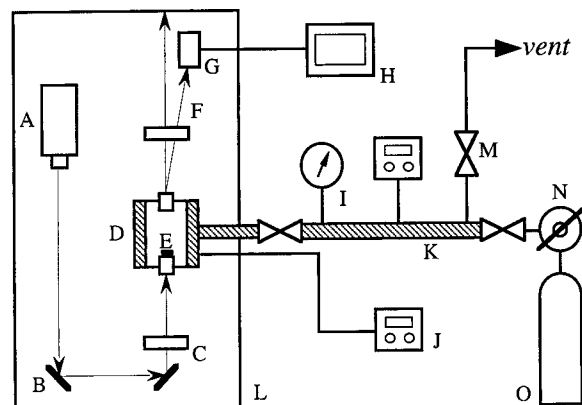


Figure 2. Schematic of high-pressure system equipped with cross-polarizers to measure the relative intensity of depolarized light: (A) He–Ne laser, (B) mirror, (C) Glen-Thompson polarizer, (D) high-pressure cell with sapphire windows, (E) thin liquid film of LCP solution, (F) scattered light, (G) photodetector, (H) photomultiplier and data acquisition, (I) pressure gauge, (J) temperature controller, (K) heating tape and insulation, (L) dark box, (M) valve, (N) pressure regulator, and (O) compressed fluid cylinder.

height. Two 0.5 in. diameter and height, cylindrical-shaped sapphire windows (Crystal Systems, Inc.; 0° flat 1 wave, tolerance ±0.001 in., 0.010 in. edge reduction) are securely held in place by stainless steel glands on either end of the cell. There is a side port in the middle of the cell for pressurization and depressurization. During experiments, the cell was positioned such that the sapphire windows were aligned vertically.

Crossed Glen-Thompson polarizers (Newport Technologies, Inc.; calcite) were placed a few inches above and below the cell, in line with the sapphire windows. A helium–neon laser (Newport U1508, class II 0.5 W) generated a beam that was directed through the first polarizer, the high-pressure cell, and the second polarizer. Approximately 3 in. above the second polarizer was a photodetector (Mettler Instruments Corp. photomultiplier 17517). Positioned to receive only scattered light, this detector generated a current proportional to the measured intensity. The high-pressure cell, laser, polarizers, and photodetector were housed inside a metal dark box.

Current from the photodetector traveled to a photomultiplier (Mettler FP80HT central processor), where it was processed relative to an initial intensity setting. Light intensity data were then stored at specific time intervals. Therefore, by recording the pressure as a function of time, it was possible to relate the intensity of scattered, depolarized light to the applied pressure. The cell, connecting lines, and valves (HIP Equipment) were tightly wrapped with heating tape and covered with a layer of insulation. The system temperature was monitored and adjusted with a Valley Forge Instruments Co. temperature controller (Model PC60405). This high-pressure system was originally used by Li and Radosz to measure pressure-induced melting and crystallization of poly(ethylene oxide)²⁴ and pressure-induced phase transitions in polymer blends.²⁵

To create a very thin liquid film, typically 6.0 μL of polymer–salt solution was pipetted onto the lower sapphire window. As illustrated in Figure 3, this window was attached to its gland, which was then resealed to the bottom end of the high-pressure cell. When the system was thermally equilibrated, and after the scattered light intensity was allowed to attain a steady value (following the relaxation of shear stresses due to the pipet delivery), compressed gas was introduced slowly at rates ranging from 0.4 to 3 bar/min to avoid shearing the liquid film. The system temperature was monitored at the compressed gas inlet line (Figure 2) and within the cell's thermocouple well (Figure 3). The pressure was measured with a US Gauge Co. pressure gauge (dial 02614) housed just prior to the cell's inlet port.

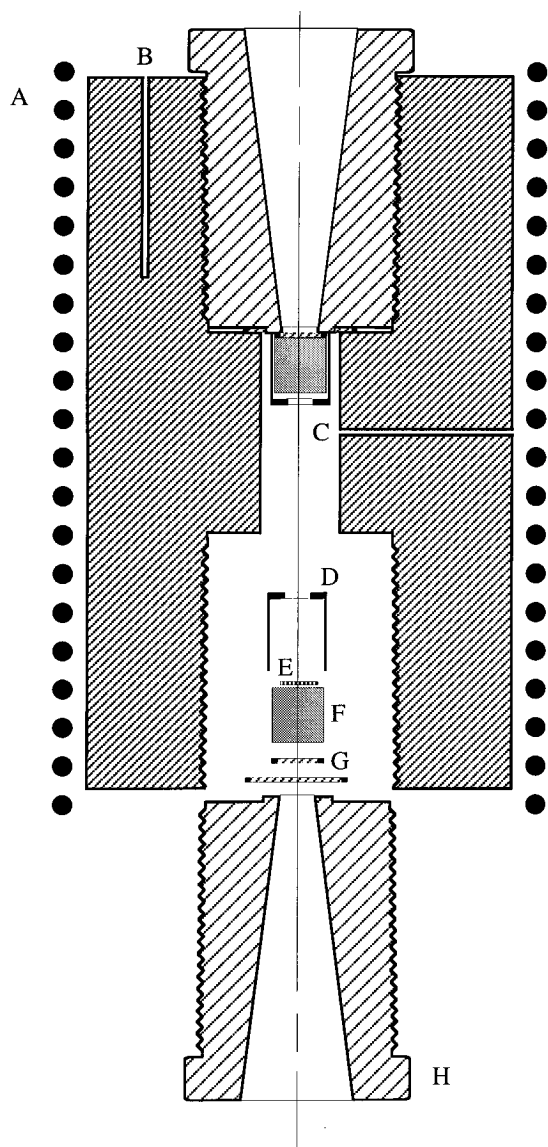


Figure 3. Cross-sectional view of high-pressure optical cell for measuring the intensity of depolarized light through an LCP liquid sample in contact with a compressed fluid: (A) electric heating tape and insulation, (B) thermocouple well, (C) pressurizing/depressurizing port, (D) brass cap, (E) LCP liquid sample, (F) sapphire window, (G) Buna-N O-rings, and (H) stainless steel gland.

Results and Discussion

Isotropic Polyamide System. Initial experiments were conducted with isotropic, 3.0 wt % PPTA-Cl solutions in DMAc (4.0 wt % LiCl) and compressed CO₂. Figure 4 shows representative results, corresponding to 6.0 μ L of this solution being delivered to the lower window of the high-pressure cell, and subsequent addition of CO₂. As suggested by Suresh *et al.*, the solubility of the polyamide in the CO₂ was considered negligible.⁷

A noteworthy feature of Figure 4 is the proximity of the low-pressure (<42 bar) intensity readings to the baseline given by the intensity of scattered light through the empty cell. This confirms the isotropy of the polymer solution.

The sharp intensity peak at ~43 bar corresponds to precipitation of polymer from solution. The presence of solid polymer on the lower window was confirmed visually immediately following the intensity peak. CO₂ dissolution into the liquid phase caused the solution to

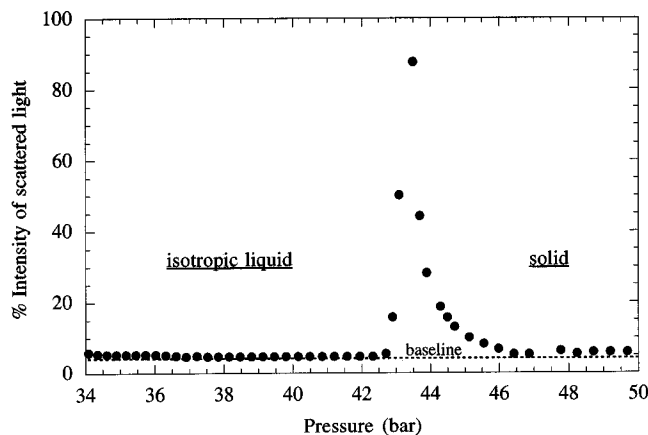


Figure 4. Percentage intensity of light scattered by 6.0 μ L of the 3.0 wt % PPTA-Cl in DMAc/LiCl (4.0 wt %) solution in contact with CO₂ at 27 °C as a function of pressure: (●) % scattered light intensity readings; (...) baseline representing intensity readings measured prior to loading the cell with the polymer solution.

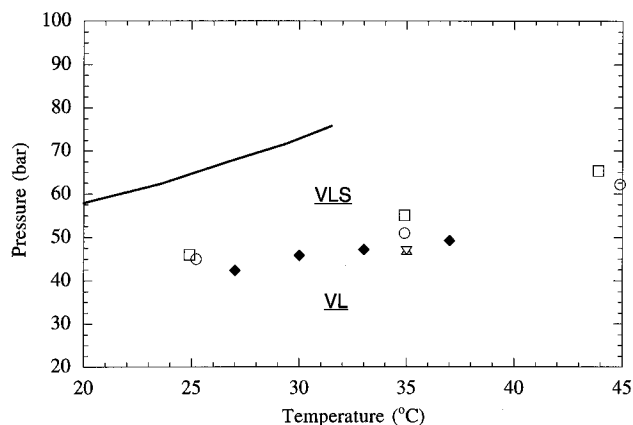


Figure 5. Equilibrium phase boundaries for various polyamide systems. Data points represent solid phase polymer precipitation boundary. VLS signifies the coexistence of vapor, liquid, and solid phases; VL indicates coexistence of vapor and liquid phases: (—) CO₂ vapor pressure curve; (◆) light scattering results from this study for 3.0 wt % PPTA-Cl in DMAc/LiCl (4.0 wt %); (Δ) Yeo *et al.* (1995), 0.1% polyamide 1 in DMAc/LiCl (4.0 wt %); (▽) Yeo *et al.* (1995), 0.1 wt % polyamide 2 in DMAc/LiCl (2.3 wt %); (□) Yeo *et al.* (1993), 0.1 wt % polyamide 8 in DMSO; (○) Yeo *et al.* (1993), 1.0 wt % polyamide 8 in DMSO.

expand and the polymer to precipitate.^{13,26} Inhomogeneities in the liquid phase due to polymer precipitation account for the rapid increase in the scattering intensity.²⁷ Immediately following the rapid intensity increase, a thin solid polymer film was observed. This film blocked light, which explains the sharp decrease in the intensity signal.²⁴

Liquid-crystalline solutions are optically anisotropic, they depolarize plane-polarized light. For anisotropic materials, the intensity of the scattered (or depolarized) light is proportional to the angle between the second polarizer, sometimes termed the analyzer, and the direction of the polymer alignment. Conversely, for isotropic materials, the scattered light intensity is not a function of polarizer alignment angle. To verify that the system was, indeed, isotropic before and after polymer precipitation, the polarizers were uncrossed and aligned parallel. No intensity change was observed.

Figure 5 depicts the nucleation boundaries for several aromatic polyamides in DMAc or dimethyl sulfoxide (DMSO). The polyamide chemical structures are given

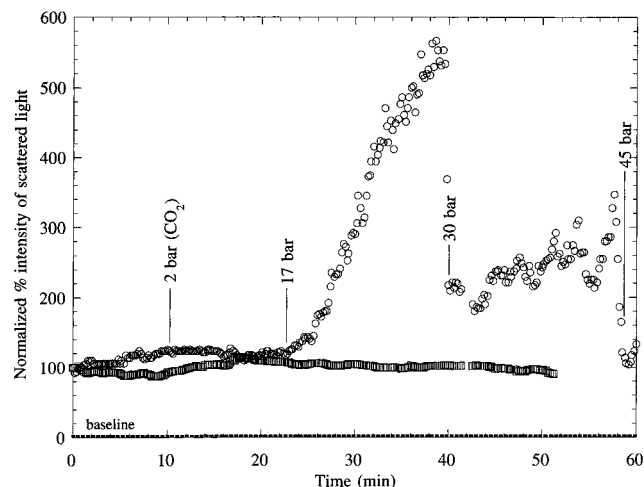


Figure 6. Normalized percentage intensity of light scattered by the anisotropic phase of the 11 wt % PPTA-Cl in DMAc/LiCl (4.0 wt %) solution as a function of time and pressure: (O) intensity readings for the polyamide system pressurized with CO₂; (□) intensity readings for the polyamide system maintained at atmospheric pressure with no CO₂ present; (...) baseline reading measured prior to loading the cell with the anisotropic solution.

in Figure 1. The filled diamonds represent the location of precipitation peaks at various temperatures. The other symbols correspond to optical view cell work of Yeo *et al.*^{12,13} and show good agreement with the measurements of this study. This suggests that light scattering is a viable means of monitoring precipitation and supports the notion of polymer precipitation caused by CO₂ dissolution and solution expansion.

Yeo *et al.*^{12,13} indicated that at sufficiently high pressures, CO₂ acts as an antisolvent toward the polyamide, causing the DMAc phase to expand and the polymer to precipitate. As noted by Yeo *et al.*¹² and illustrated in Figure 5 by the proximity of experimental data points, the threshold polymer nucleation pressure, or cloud point, is relatively independent of polymer concentration in the range 0.1–3.0 wt % and of substitutional groups. Upon continued pressurization at 35 °C, Yeo *et al.* observed that LiCl precipitation occurred above 50 bar.¹³ The nucleation of LiCl due to the presence of CO₂ was verified in separate view cell experiments similar to the ones conducted by Yeo *et al.*^{12,13} For 4.0 wt % LiCl in DMAc solutions (with no polymer present) at 30 °C, CO₂ caused LiCl to precipitate from DMAc at 51 bar.

Anisotropic Polyamide System. A second series of experiments involved contact between CO₂ or argon and the lower, anisotropic phase of an 11 wt % PPTA-Cl in DMAc (4.0 wt % LiCl) biphasic solution. The top phase of this biphasic solution was isotropic. Care was taken to pipet only the lower phase from the biphasic solution to the sapphire window. To compare trends between different experiments, the intensity readings of scattered light were normalized so that a steady state reading at the beginning of each run defined the 100% marks.

Figure 6 illustrates a typical scattering intensity response as a function of time; the circles depict the response to the compressed CO₂, while the squares represent the control run at atmospheric pressure, with no CO₂ added. The intensity readings for the control run remained constant, with only slight fluctuations due to the dynamic nature of the alignment of polymer chains relative to the fixed position of the cross-

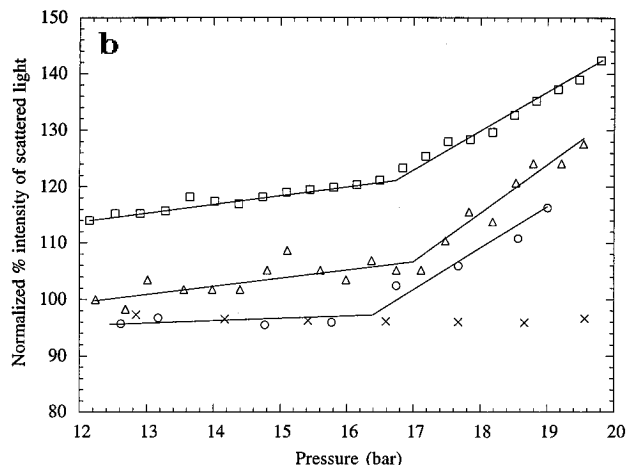
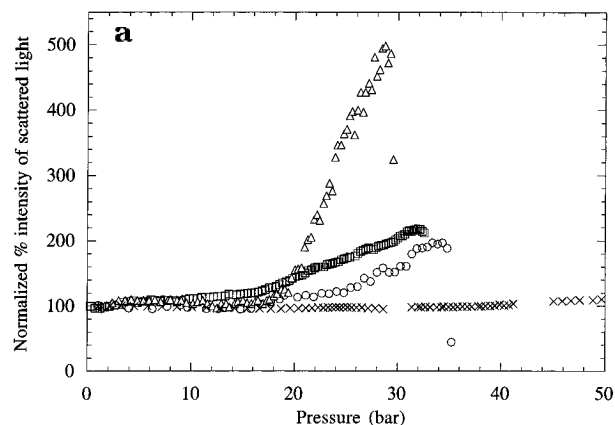


Figure 7. Normalized percentage intensity readings of light scattered by 11 wt % PPTA-Cl in DMAc/LiCl (4.0 wt %) solutions: (Δ, □, O) duplicate runs for polyamide solutions at 27 °C in contact with compressed CO₂; (x) polyamide solution at 29 °C in contact with compressed argon. (a) The differences in the magnitude of light scattered between duplicate runs illustrate that the polymer alignment upon loading the cell is arbitrary relative to the position of the cross-polarizers. (b) The onset of the increase in scattering intensity at ~17 bar is reproducible among duplicate experiments.

polarizers. In contrast, pressurization with CO₂ caused a sharp rise in the intensity of scattered light at 17 bar. This rise continued across a pressure range of ~13 bar. Additional experiments at 27 °C confirmed that this intensity rise was sustained through at least a 15 bar range. Three such control runs are depicted in Figure 7.

Upon further increasing the pressure, a sharp drop in intensity was observed (e.g., around 30 bar for this particular run). As confirmed visually, this corresponds to polymer precipitation, again due to solution expansion caused by CO₂ dissolution, as in the isotropic 3.0 wt % polyamide system. For the anisotropic 11 wt % polymer experiments, as expected, the pressure required for polyamide nucleation was less than that necessary for precipitation from the isotropic 3.0 wt % polyamide systems. At 45 bar, another sharp decrease in the intensity of scattered light was observed. It corresponds to the precipitation of LiCl.

Results for several experiments at 27 °C are illustrated in Figure 7. It can be seen from Figure 7b that the pressure at which the intensity first rises is reproducible. The scattering intensity is proportional to the angle between the analyzer and the direction of polymer alignment. Therefore, the difference in the magnitudes of scattered light between the three runs,

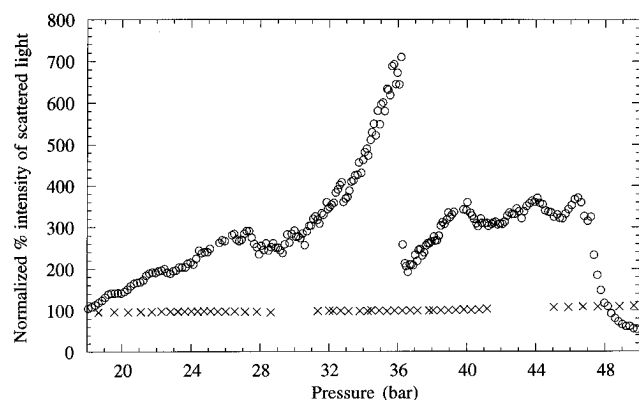


Figure 8. Normalized percentage intensity of light scattered by anisotropic phase of the 11 wt % PPTA-Cl in DMAc/LiCl (4.0 wt %) solution: (○) polyamide solution at 30 °C in contact with compressed CO₂; (×) polyamide solution at 29 °C in contact with compressed argon.

Table 1. Transition Temperatures and Pressures for the Anisotropic Phase of an 11 Wt % PPTA-Cl in DMAc (4.0 Wt % LiCl) Solution Exposed to Compressed CO₂

temp (°C)	pressure (bar)		
	initial rise	polymer nucleation	salt precipitation
27	17	32	45
28	17	33	46
30	18	36	47

as depicted in Figure 7a, merely reflects the fact that polymer alignment upon loading the high-pressure cell is arbitrary relative to the orientation of the cross-polarizers.

The CO₂ pressurization rates for the experimental runs illustrated in Figure 7b were ~1 bar/min, small enough to avoid disrupting or shearing the liquid film. The location of the onset of the increase in the intensity of scattered light was unaffected by changes in the pressurization rate, as shown in Figure 7b. This suggests that the pressurization rate was always small enough to allow dissolution and equilibration of the CO₂ in the liquid phase.

Experiments were conducted with the same anisotropic LCP solution and compressed argon. Under the conditions explored, argon did not act as an antisolvent toward DMAc solutions. As expected and illustrated in Figure 7, argon served only to pressurize the cell. No rise in scattering intensity occurred, indicating that pressure alone did not cause the behavior shown in Figures 6 and 7. Furthermore, the cell was filled in separate experiments with CO₂ and argon to pressures of ~56 bar in the absence of polymer solution; no changes in scattering intensity were observed.

Figure 8 depicts analogous results for a run at 30 °C. The dramatic drops in intensity at 36 and 47 bar again represent polymer and salt nucleation, respectively. Table 1 summarizes results at three different temperatures; notice in each case that the pressures required for polymer and salt nucleation increased with temperature (as also illustrated in Figure 5 for the isotropic polyamide system). This follows from the facts that the solubility of a solid in a liquid increases with temperature, and, conversely, that the solubility of a gas in a liquid decreases with temperature.

The notion that nucleation of solid polymer (and thus the introduction of inhomogeneities in the liquid phase) caused the intensity rise at 17 bar was ruled out by the fact that the increase in scattering intensity was

sustained for ~15 bar. As illustrated in Figure 4, solid polymer precipitation at 27 °C was rapid and essentially complete within a narrow (2 bar) pressure interval.

The intensity of scattered and depolarized light is directly proportional to the birefringence of the polymer system. Thus, the key to understanding the experimental observations lies in identifying the mechanisms that can lead to altered polyamide birefringence levels. One potential mechanism is the direct interaction between the aromatic polyamide chains and CO₂ molecules, leading to polyamide chain stiffening. Literature results, however, suggest that chain stiffening due to polyamide-CO₂ interactions is unlikely.⁷ Polyamides exhibit strong intra- and intermolecular hydrogen-bonding, leading to the formation of networks.²⁸ Therefore, it is unlikely that polyamide-CO₂ interactions caused the observed behavior or disrupted the inter-chain hydrogen bonds present in the PPTA-Cl.⁷

A more likely interpretation for the increase in birefringence involves phase separation as a consequence of CO₂ dissolution. In this interpretation, the dissolution of CO₂ in DMAc causes a phase split into polymer-rich (anisotropic) and polymer-lean (isotropic) phases, in analogy with the observations of Suresh *et al.*⁷ for the Nylon 6, TF₂OH, and CO₂ system. As a consequence of the phase split, the polymer concentration in the anisotropic phase increases. The lyotropic mixture therefore achieves higher directional order, which is observed by the increase in light scattering. For the 27 °C experiments, the onset of this transition would occur at 17 bar. Thereafter, with increasing pressure, the polymer concentration in the anisotropic phase continues to increase as DMAc becomes gradually more enriched with CO₂, the antisolvent, until precipitation occurs at 32 bar. This interpretation is speculative but consistent with observations and calculations for a similar system.⁷ The complexity of our quaternary system, consisting of a lyotropic liquid-crystalline polymer, an organic solvent, an electrolyte, and a compressed fluid, makes phase equilibria calculations considerably more challenging. Future work with a high-pressure optical view cell will attempt to verify the polymer solution phase separation experimentally.

Conclusion

The mechanical strength of solid state fibers, wet-spun from anisotropic solutions, is intimately related to the structure developed in the liquid-crystalline solution.²⁹ The more ordered the liquid-crystalline structure, the higher the mechanical strength of solid state fibers becomes. Our results suggest that compressed antisolvents may increase anisotropy within lyotropic LCP systems by concentrating and fractionating polymer species. Moderate changes in pressure affect the dissolution of the compressed gas antisolvent and the subsequent expansion of the liquid phase. Thus, as a consequence of the high compressibility of supercritical antisolvents, small changes in pressure may enable fine control of polymer solution microstructure.

Acknowledgment. P.G.D. gratefully acknowledges the financial support of the National Science Foundation, Interfacial, Transport, and Separations Processes Program (Grant CTS-9321978); the Air Force Office of Scientific Research (Grant F49620-93-0040); and the U.S. Department of Energy, Office of Basic Energy Sciences, Division of Chemical Sciences (Grant DE-FG02-

87ER13714). The authors gratefully acknowledge Sabine Mayer and Dr. Alfred G. Oertli for synthesizing the PPTA-Cl.

References and Notes

- (1) Roviello, A.; Sirigu, A. *J. Polym. Sci.: Polym. Lett.* **1975**, *13*, 455.
- (2) Ober, C. K.; Weiss, R. A. *Current Topics in Liquid-Crystalline Polymers*; ACS Symposium Series 260; ACS: Washington, DC, 1984.
- (3) Jaffe, M. High Modulus Polymers. In *Encyclopedia of Polymer Science and Engineering*; Mark, H. F., Bikales, N. M., Overberger, C. G., Menges, G., Kroschwitz, J. I., Eds.; Wiley Interscience: New York, 1987.
- (4) Northolt, M. G. Aramids—Bridging the Gap Between Ductile and Brittle Reinforcing Fibers. In *Recent Advances in Liquid Crystalline Polymer*; Chapoy, L. L., Ed.; Elsevier Applied Science Publishers: London, 1985.
- (5) Collings, P. J. *Liquid Crystals: Nature's Delicate Phase of Matter*; Princeton University Press: Princeton, NJ, 1990.
- (6) National Materials Advisory Board: Committee on Liquid Crystalline Polymers. *Liquid Crystalline Polymers*; National Academy Press: Washington, DC, 1990.
- (7) Suresh, S. J.; Enick, R. M.; Beckman, E. J. *Macromolecules* **1994**, *27*, 348.
- (8) Huang, S. H.; Radosz, M. *Ind. Eng. Chem. Res.* **1990**, *29*, 2284.
- (9) Huang, S. H.; Radosz, M. *Ind. Eng. Chem. Res.* **1991**, *30*, 1994.
- (10) McHugh, M. A.; Guckes, T. L. *Macromolecules* **1985**, *18*, 674.
- (11) Seckner, A. J.; McClellan, A. K.; McHugh, M. A. *AIChE J.* **1988**, *34*, 9.
- (12) Yeo, S.-D.; Debenedetti, P. G.; Radosz, M.; Giesa, R.; Schmidt, H.-W. *Macromolecules* **1995**, *28*, 1316.
- (13) Yeo, S.-D.; Debenedetti, P. G.; Radosz, M.; Schmidt, H.-W. *Macromolecules* **1993**, *26*, 6207.
- (14) Dixon, D. J.; Johnston, K. P.; Bodmeier, R. A. *AIChE J.* **1993**, *39*, 127.
- (15) Randolph, T. W.; Randolph, A. D.; Mebes, M.; Yeung, S. *Biotechnol. Prog.* **1993**, *9*, 439.
- (16) Hatke, W.; Land, H.-T.; Schmidt, H.-W.; Heitz, W. *Makromol. Chem., Rapid Commun.* **1991**, *12*, 235.
- (17) Hatke, W.; Schmidt, H.-W. *Polym. Prepr., Am. Chem. Soc. Div. Polym. Chem.* **1991**, *32*, 214.
- (18) Hatke, W.; Schmidt, H.-W. *Makromol. Chem., Macromol. Symp.* **1991**, *50*, 41.
- (19) Kiamos, A. A.; Donohue, M. D. *Macromolecules* **1994**, *27*, 357.
- (20) Kumar, S. K.; Chabria, S. P.; Reid, R. C.; Suter, U. W. *Macromolecules* **1987**, *20*, 2250.
- (21) Bair, T. I.; Morgan, P. W.; Killian, F. L. *Macromolecules* **1977**, *10*, 1396.
- (22) Kwolek, S. L.; Morgan, P. W.; Schaefgen, J. R. Liquid Crystal Polymers. In *Encyclopedia of Polymer Science and Engineering*; Mark, H. F., Bikales, N. M., Overberger, C. G., Menges, G., Kroschwitz, J. I., Eds.; Wiley Interscience: New York, 1987.
- (23) Akki, R.; Desai, P.; Abhiraman, A. S. *J. Appl. Polym. Sci.* **1994**, *54*, 1263.
- (24) Li, W.; Radosz, M. *Macromolecules* **1993**, *26*, 1417.
- (25) Li, W.; Radosz, M. *Polym. Prepr., Am. Chem. Soc. Div. Polym. Chem.* **1992**, *33* (2), 422.
- (26) Yeo, S.-D.; Lim, G.; Debenedetti, P. G.; Bernstein, H. *Biotechnol. Bioeng.* **1993**, *41*, 341.
- (27) van de Hulst, H. C. *Light Scattering by Small Particles*; Dover Publications, Inc.: New York, 1981.
- (28) Kohan, M. I. *Nylon Plastics*; John Wiley and Sons: New York, 1973.
- (29) Bheda, J.; Fellers, J. F.; White, J. L. *J. Appl. Polym. Sci.* **1981**, *26*, 3955.

MA9518518